# Jet flow aeroacoustics at Re=93000: comparison between experimental results and numerical predictions


L. Bricteux , M. Duponcheel , G. Winckelmans

*Institute of Mechanics, Materials and Civil Engineering (iMMC)*

*Université catholique de Louvain 1348, Louvain la Neuve, Belgium.*

C. Schram

*von Karman Institute for Fluid Dynamics, Chaussée de Waterloo 72, 1640 Rhode-st-Genese, Belgium*


## I. Introduction

This paper is concerned with the numerical prediction of the noise of a subsonic jet at a high Reynolds number: $Re = \frac{U\,D}{\nu} = 93000$, where $U$ is the jet velocity, $\nu$ is the kinematic viscosity and $D = 2R$ is the diameter of the nozzle. The simulated flows correspond to the experiment performed by Schram et al.[9] This experiment consists in a low Mach number excited jet, and is measured using particle image velocimetry (PIV). The pairing of vortex rings is one of the basic mechanisms for sound production in subsonic free jets. Based on the description of the experiment, we consider the simulation of two flow configurations:

1. The DNS (Direct Numerical Simulation) of the pairing of an isolated vortex pair using, as initial condition, a PIV field extracted from the experimental jet.
2. The DNS of the jet with the same physical parameters as those of the experiment.

The acoustic source terms are evaluated using the DNS fields computed for the two cases and compared to those of the experiment. The study performed here is in the continuation of the work of Detandt et al.,[2] who performed the comparison at a moderate Reynolds number, $Re = 14000$. The paper is organized as follows: in the second section, the numerical approach used to solve these two problems is presented; in the third section the conservative aeroacoustic analogy is presented; then the results obtained for case 1 and case 2 are discussed.

## II. Numerical method

The DNS of the considered flows are performed using a finite difference code which solves the incompressible axisymmetric Navier-Stokes equations in vorticity-stream function formulation. This amounts to solve one evolution equation for the tangential component of the vorticity $\omega_\varphi = \frac{\partial u_r}{\partial z} - \frac{\partial u_z}{\partial r}$:

$$\frac{\partial \omega_\varphi}{\partial t} + \frac{1}{r}\frac{\partial \psi}{\partial r}\frac{\partial \omega_\varphi}{\partial z} - \frac{1}{r}\frac{\partial \psi}{\partial z}\frac{\partial \omega_\varphi}{\partial r} + \frac{\omega_\varphi}{r^2}\frac{\partial \psi}{\partial z} = \nu\left(\frac{\partial^2 \omega_\varphi}{\partial z^2} + \frac{\partial^2 \omega_\varphi}{\partial r^2} + \frac{1}{r}\frac{\partial \omega_\varphi}{\partial r} - \frac{\omega_\varphi}{r^2}\right) \tag{1}$$

From incompressibility,the velocity is obtained from a streamfunction $\psi$:

$$u_z = \frac{1}{r}\frac{\partial \psi}{\partial r}, \quad u_r = -\frac{1}{r}\frac{\partial \psi}{\partial z}\,. \tag{2}$$

This then leads to the following equation for $\psi$:

$$\frac{\partial^2 \psi}{\partial z^2} + \frac{\partial^2 \psi}{\partial r^2} - \frac{1}{r}\frac{\partial \psi}{\partial r} = -r\omega_\varphi\,. \tag{3}$$

The derivatives in the convective term are computed using a fourth order compact Padé scheme to limit dispersion errors. The diffusive term is evaluated using second order finite differences. The time stepping is performed using a fourth order Runge-Kutta scheme in order to capture accurately the time variations of the acoustic source term. The Poisson equation is solved efficiently using a parallel geometric multigrid approach. The Poisson equation is solved at each Runge Kutta substep to ensure the fourth order time accuracy of the diagnostics. The boundary conditions are also updated at each substep. The fluid flow is very well resolved and the mesh based Reynolds number stays very low during the simulations. The code was validated by comparing its results to those obtained in Verzicco et al.[10] and Iafrati et al[3] for the case of leapfrogging vortex rings. The run were performed on 48-core shared memory parallel machines .

# III. Conservative acoustic analogy

The sound produced by leapfrogging vortex rings extracted from a jet is predicted using a conservative formulation of the vortex sound theory as described by Schram et al.[9] This analogy is less sensitive to errors in the flow data than the original formulations of Powell[7] and Mohring[6] from which it is derived. For a DNS, which also mimics a perfect PIV, this analogy should thus provide good results. The numerical sound prediction will be compared to that of the experiment. It is expected that, at such a high Reynolds number, the conservative formulation (based strongly on the kinetic energy conservation) will provide realistic acoustic results. In this analogy, the acoustic pressure fluctuations are given by:

$$p'(\mathbf{x},t) = \frac{\rho_0}{4\,c_0^2\,|\mathbf{x}|}\frac{d^2Q}{dt^2}\left(\cos^2(\alpha) - \frac{1}{3}\right)\,, \tag{4}$$

where the fluid density is $\rho_0$ and the speed of sound is $c_0$. The distance to the listener is $|\mathbf{x}|$ and the directivity angle is written $\alpha$. The acoustic pressure depends on the second derivative of the following source term:

$$Q = 3\int_S \omega_\varphi\, u_r\,(z - z_0)\; r\,dr\,dz\,. \tag{5}$$

This source term depends on the vorticity, which is accurately captured by the present numerical approach, and it also depends on the centroid of the vortex system defined by Lamb[5] :

$$z_0 = \frac{\int_S \omega_\varphi\, z\, r^2\,dr\,dz}{\int_S \omega_\varphi\, r^2\,dr\,dz}\,. \tag{6}$$

One of the strength of the analogy given by Eq. (4) is that it involves only a second order time derivative $Q''$. Recall that an analogy like that of Mohring involves a third order derivative which is far more difficult to compute with noisy signals.

# IV. Case I: pairing of isolated vortex rings

## A. Description of the case

The computational domain dimensions are $L_z = 8R$ and $L_r = R_{max} = 4R$. The grid resolution is: $n_z = 2048$ and $n_r = 1024$. It is assumed that the vortex rings evolve in an unbounded space. The boundary condition on the stream function to be applied for swirl free axisymmetric flow is obtained by the Biot-Savart law :

$$\psi(z,r) = \frac{r}{4\,\pi}\int_{-\infty}^{\infty}\int_{-\infty}^{\infty} r'\,\omega_\varphi(z',r')\int_0^{2\pi}\frac{\cos(\theta')}{\sqrt{(z-z')^2 + r^2 + r'^2 - 2r\,r'\cos(\theta')}}\,d\theta'\,dr'\,dz' \tag{7}$$

The evaluation of this integral is computationally intensive. Iafrati et al.[3] obtained a fourth order asymptotic expansion of this integral :

$$\begin{aligned}\psi^{(4)}(z,r) \;=\; & \frac{r^2}{4\,|\mathbf{z}|^3}\int_{-\infty}^{\infty}\int_{-\infty}^{\infty}\left[1 + 3\frac{z}{|\mathbf{z}|^2}z' - \frac{3}{2}\left(1 - 5\frac{z}{|\mathbf{z}|^2}\right)z'^2 - \frac{3}{2}\frac{1}{|\mathbf{z}|^2}\left(1 - \frac{5}{4}\frac{r^2}{|\mathbf{z}|^2}\right)r'^2\right. \\ & \left.-\frac{5}{2}\frac{z}{|\mathbf{z}|^4}\left(3 - 7\frac{z^2}{|\mathbf{z}|^2}\right)z'^3 - \frac{15}{2}\frac{z}{|\mathbf{z}|^4}\left(1 - \frac{7}{4}\frac{r^2}{|\mathbf{z}|^2}\right)r'^2\,z'\right] r'^2\omega_\varphi(r',z')\,dr'\,dz'\end{aligned} \tag{8}$$

The streamfunction is thus evaluated using this expansion on $r = R_{max},\ z = -2\,D,\ z = 2\,D$, while, on the symmetry axis $r = 0$, one sets $\psi = 0$. The vorticity is set to $\omega_\varphi = 0$ on the whole boundary. The surface integral given by Eq. 8 is evaluated at each Runge Kutta substep to ensure the fourth order time accuracy of the scheme. It is also worth to stress that the size of the domain is large enough to minimize boundary condition effects as illustrated in Fig. 1.

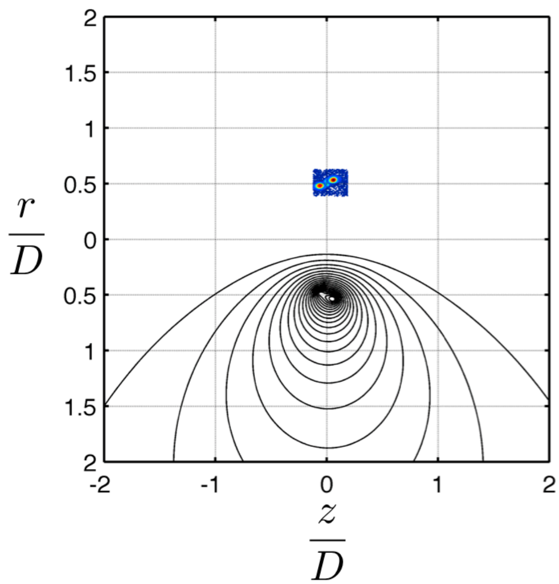


**Figure 1. Computational domain used for the DNS and initial vorticity field of an isolated vortex pair extracted from PIV (top); streamfunction computed using the multigrid Poisson solver and the multipole expansion given by Eq. 8 as boundary condition on $\psi$ (bottom).**

## B. Results

A visualization of the pairing is provided in Fig. 4. One observe the leapfrogging of the vortex rings which evolve under their own dynamics. The vorticity field obtained for the isolated pairing is also displayed at six different times. The evolution is synchronized to the vortex pairing time $t_0$:

$$\phi = \frac{2\pi\, U\, St}{D}\,(t - t_0)\ , \tag{9}$$

where $St = 3.01$ is the Strouhal number of the experimental jet acoustic excitation. The phase $\phi = 0$ is set to correspond to the instant at which the leading and trailing rings are coplanar.This is known to correspond to the peak acoustic emission.[4] As can be observed in Fig. 2, the kinetic energy is conserved during the pairing process of the vortex rings. This legitimates the use of an acoustical analogy based on energy conservation. It is important to note that the numerical integration rule chosen to evaluate the diagnostics is of primary importance. In the first part of this investigation, the Simpson rule was used. Using this rule allows to have a fourth order convergence but leads to strong oscillations in the diagnostics. This is the reason why a simple second order trapezoidal rule was chosen. One also observe in Fig. 3 that the circulation is also very well conserved during the process. The level obtained is in good agreement with that obtained in the experiment.The linear impulse is also correct as showed in Fig. 5. The source term defined in the classical Mohring analogy,

$$Q_M = \int \omega_\varphi r^2\, z\, dr\, dz \tag{10}$$

is also plotted in Fig. 6 and its evolution agrees very well with the experimental data. Finally, we display the second time derivative of the source term obtained with the conservative formulation $Q''$ in Fig. 6. The amplitude of this term agrees fairly with the experimental results but the time variation of the signal is not correct. This may be due to the fact that the dynamics of a pair of vortex rings is not the same as that of a full jet, i.e, the isolated pair does not feel the influence of the rest of the jet. This is the reason why it is proposed, in the next section, to evaluate this acoustic source term for a pair of vortex rings issued form a complete jet simulation.

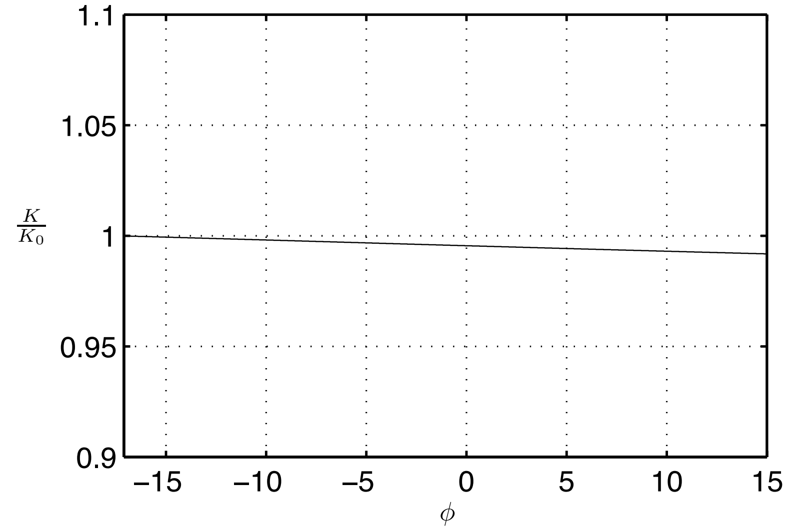


**Figure 2. Evolution of the kinetic energy $K = \frac{1}{2}\int \psi\omega_\varphi \, dV$ for the vortex ring pair. $K_0$ is the kinetic energy of the initial PIV field.**

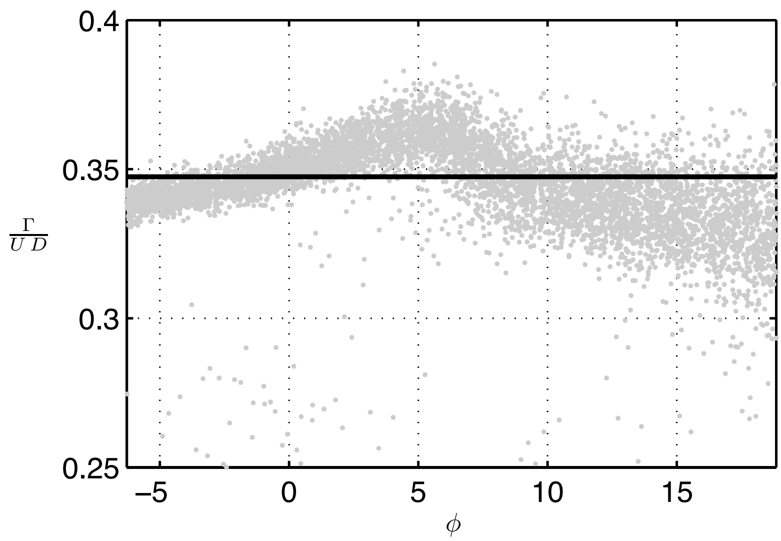


**Figure 3. Evolution of the circulation $\Gamma$ computed for the vortex ring pair: DNS (solid), experimental data (grey bullets).**

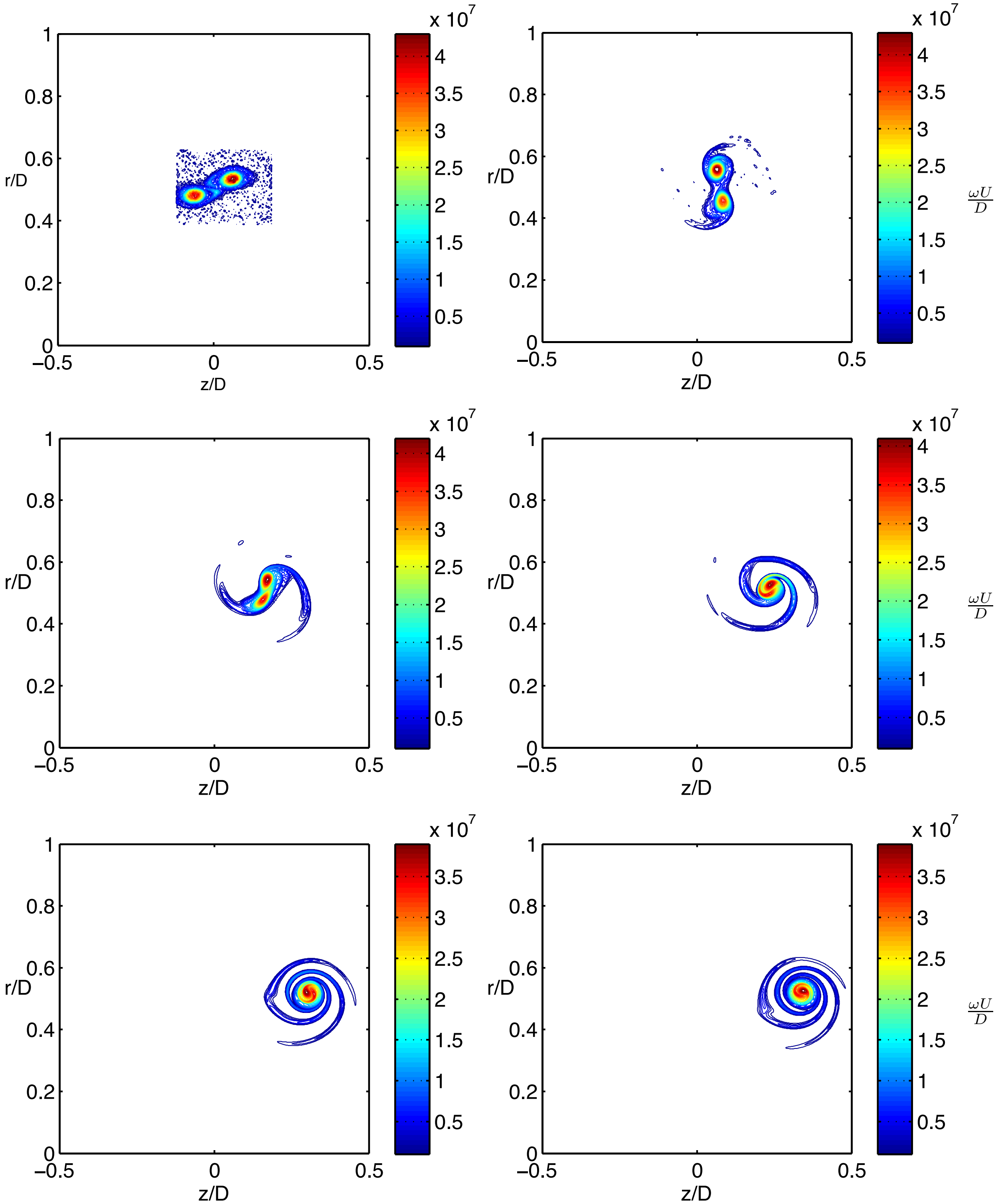


**Figure 4. Evolution of the vorticity field for the isolated vortex rings at different phases: $\phi = -5.52$ (PIV vorticity field), $\phi = 0.79$, $\phi = 10.25$, $\phi = 16.6$, $\phi = 22.9$ and $\phi = 26.0$.**

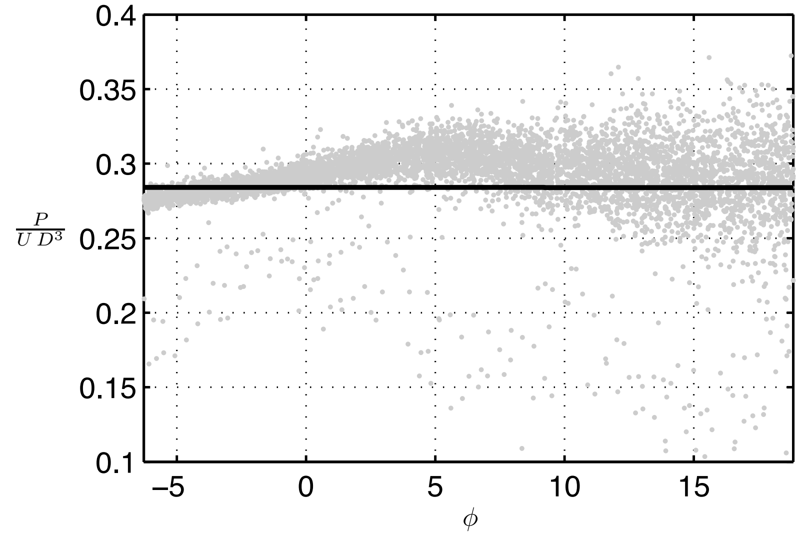


**Figure 5. Evolution of the linear impulse $P = \pi \int \omega_\varphi\, r^2\, dr\, dz$ computed for the isolated vortex ring pair: DNS (solid), experimental data (grey bullets).**

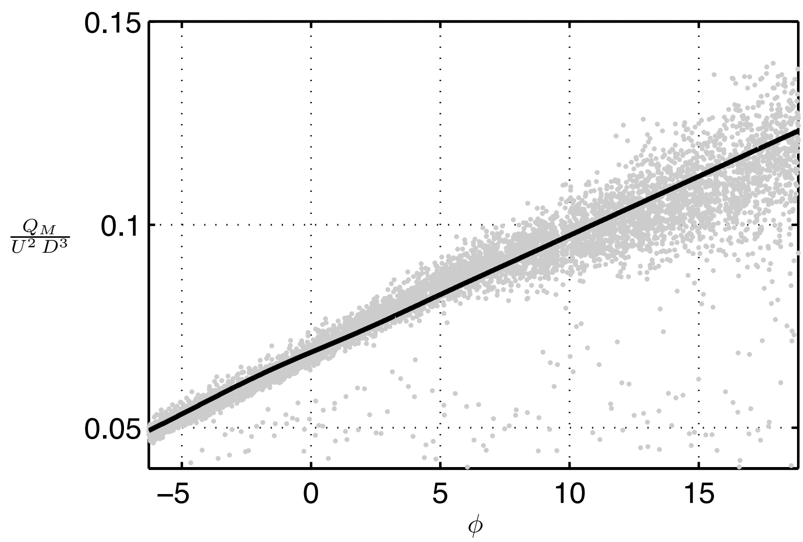


**Figure 6. Evolution of the Mohring source term $Q_M = \int \omega_\varphi r^2\, z\, dr\, dz$ computed for the isolated vortex ring pair: DNS (solid), experimental data (grey bullets).**

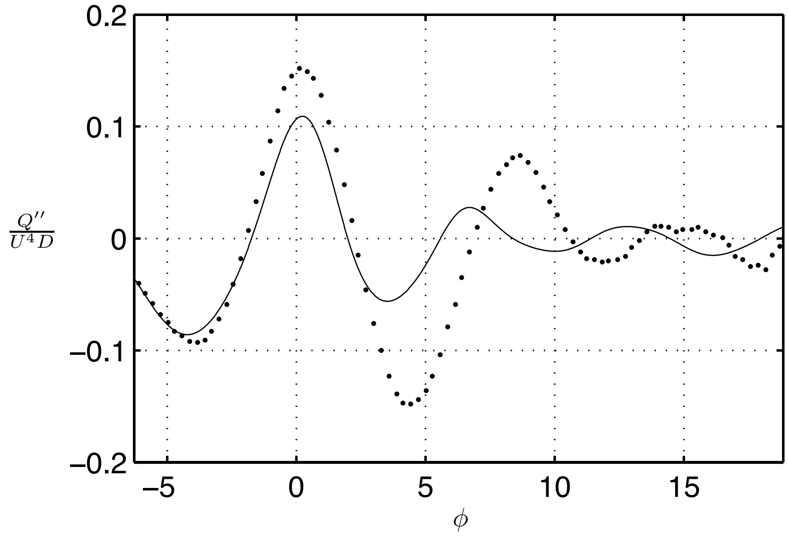


**Figure 7. Acoustic source term for the conservative analogy: experimental results (bullets), DNS of the isolated vortex pairing with a PIV initial condition (solid).**

## V. Case II: pairing of vortex rings within a complete jet

### A. Description of the case

The DNS of the jet is performed using the same parameters as those of the experiment. It is expected to obtain better acoustic results than with isolated vortex rings since their dynamics is influenced by the other vortex rings of the jet. The Mach number ($M = 0.1$) is low so that the flow is assumed to be incompressible. The inlet boundary conditions are imposed so that the jet is excited trough a small amplitude ($\epsilon$) temporal fluctuation which is superposed to an axisymmetric profile. Written in cylindrical coordinates $(r, \varphi, z)$, the inlet velocity profile is given by:

$$u_z(0,r,t) = \frac{U}{2}\left(1 + \epsilon\,\sin\left(\frac{2\,\pi\,St\,U\,t}{D}\right)\right)\left(1 + \tanh\left(\frac{\theta\,R}{4}\left(\frac{R}{r} - \frac{r}{R}\right)\right)\right) . \tag{11}$$

The exit momentum thickness value is $\theta = 0.0042\,D$ and the Strouhal number value is $St = 3.01$. Integrating the velocity profile along the radial direction allows to obtain the streamfunction profile at the inlet:

$$\psi(0,r,t) = \int_0^r u_z(0,r',t)\,r'dr' . \tag{12}$$

This velocity profile also leads to a vorticity profile obtained as:

$$\omega_\varphi(0,r,t) = -\frac{U\,\theta\,R}{8}\left(1 + \epsilon\,\sin\left(\frac{2\,\pi\,St\,U\,t}{D}\right)\right)\left(1 - \tanh\left(\frac{\theta\,R}{4}\left(\frac{R}{r} - \frac{r}{R}\right)\right)^2\right)\left(-\frac{R}{r^2} - \frac{1}{R}\right) . \tag{13}$$

The set of conditions to apply on the rest of the boundary are taken as:

$$\begin{aligned} \omega_\varphi(z,0,t) &= 0\,, & \psi(z,0,t) &= 0\,, \\ \omega_\varphi(z,R_{max},t) &= 0\,, & \psi(z,R_{max},t) &= \psi(0,R_{max},t)\,, \\ \frac{\partial\omega_\varphi}{\partial z}(L_z,r,t) &= 0\,, & \frac{\partial\psi}{\partial z}(L_z,r,t) &= 0\,. \end{aligned} \tag{14}$$

The computational domain dimensions are $L_z = 10R$ and $R_{max} = 5R$. The grid resolution is such that: $n_z = 4096$ and $n_r = 2048$.

### B. Results

A snapshot of the flow is provided for visualization purposes in Fig. 9. The high resolution allows to capture very fine vortical structures and filaments. As the vortex pairing is the most dominant source of noise, we compute the source term integrals on a window which is convected at a constant speed (here $U_w = 0.57\,U$, the same velocity as that used in the experiment) and follows the vortices during their pairing. This is equivalent to evaluating the source term in the whole domain of the isolated leapfrogging vortex rings. When the flow becomes complex, some vorticity may enter the window or leave it. This leads to severe spurious oscillations in the derivatives of the acoustic terms. This strategy allows to compute the acoustic source term displayed in Fig. 8. A very good agreement between the source term obtained experimentally and that provided by the DNS is observed. However, one cannot predict the source term over a sufficient period of time to compute acoustic spectra. This is due to the spurious oscillations induced by vorticity entering and leaving the integration window.

The basic tracking algorithm was modified to better isolate the vortex pair and thus avoid spurious oscillations. The vorticity in the moving window is filtered to remove the vorticity which does not belong to the tracked vortices. This is achieved by considering that the vortex pair is a compact patch of vorticity larger than a definite threshold and which is connected to the local vorticity maximum of the moving window. Practically, the patch is obtained, starting from the maximum of vorticity, by adding successively all the neighbor cells with a vorticity above the threshold. The boundary of the patch is then smoothed. The efficiency of the technique is shown in Fig. 10 where a snapshot of the vorticity field is shown along with the extracted merging vortex pair. The global flow diagnostics, namely the circulation and the impulsion of the extracted vortex pair are displayed in Fig.11 and Fig. 12. The agreement with the experimental values is good. The acoustic source term evolution computed with the improved tracking algorithm is reported in Fig. 13. A good agreement between the numerical and the experimental results is also observed. In this case, a larger part of the signal can be recovered compared to the basic tracking algorithm. These results show the importance of the vortex tracking algorithm and that the present approach is correct to predict vortex sound.

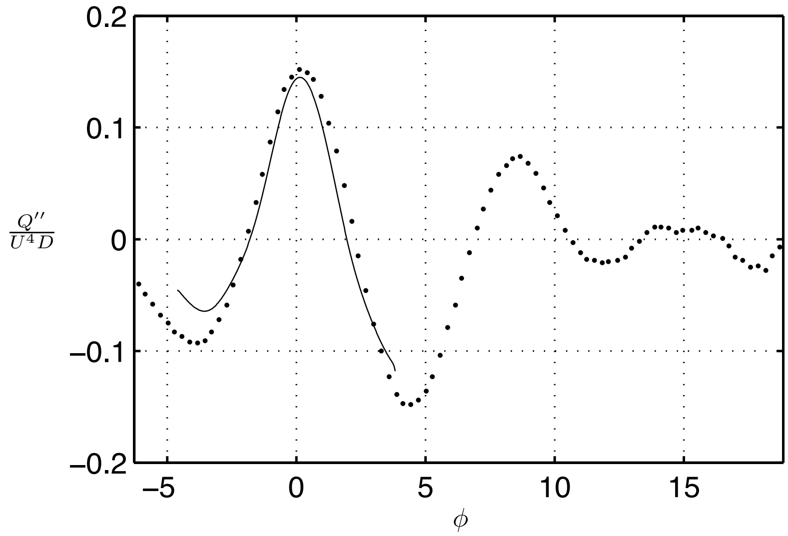


**Figure 8. Acoustic source term evaluated using the basic tracking algorithm for the conservative analogy: experimental results (bullets), DNS of the jet (solid).**

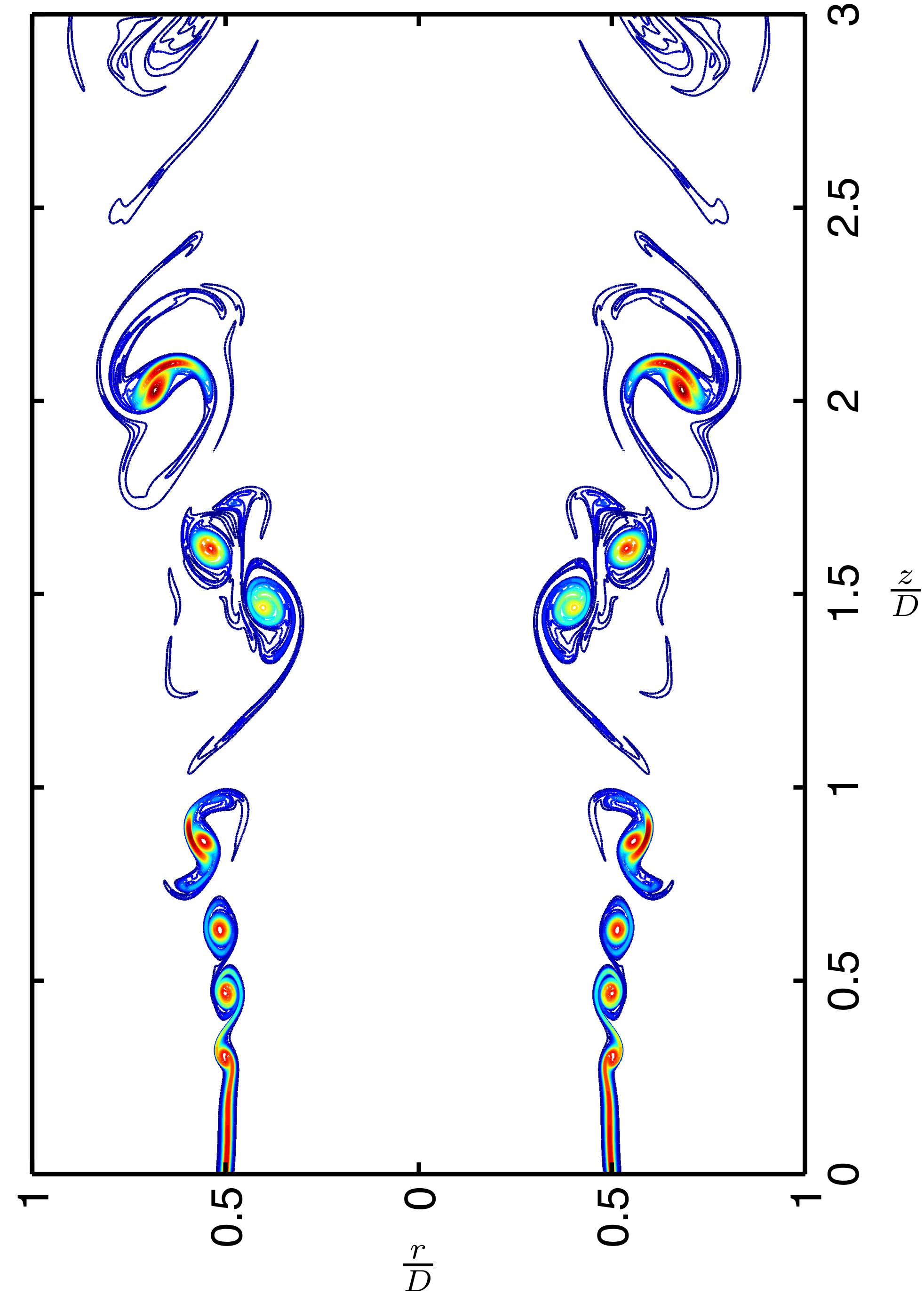


**Figure 9. Visualization of the jet: snapshot of the vorticity field. The computational domain is cropped to $[3D \times 1D]$. The domain is duplicated below the symmetry axis.**

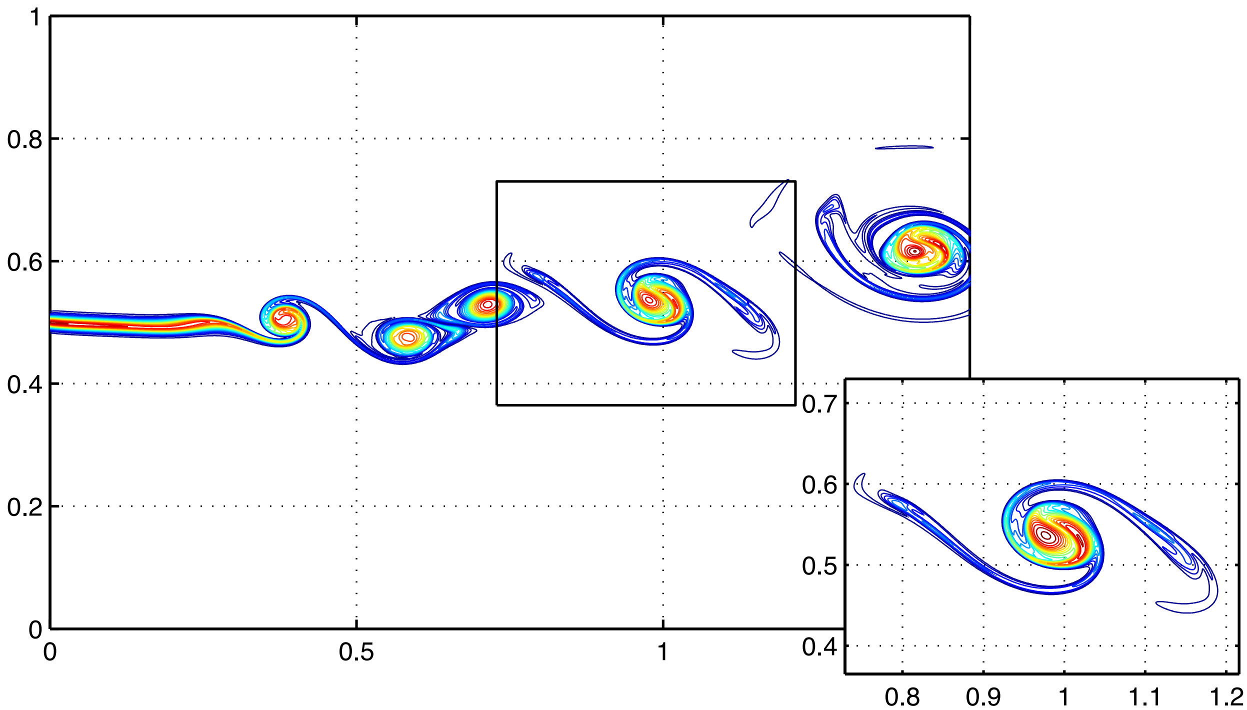


**Figure 10. Snapshot of the vorticity field for case 2 with moving integration window. The effect of the improved eduction technique is illustrated in the lower window where the unwanted vorticity features are discarded.**

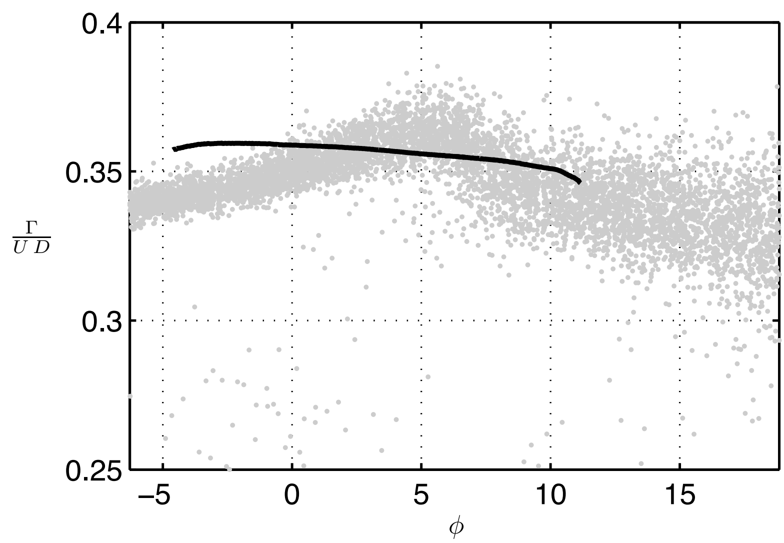


**Figure 11. Evolution of the circulation $\Gamma$ : experimental results (grey bullets), DNS of the jet (solid)**

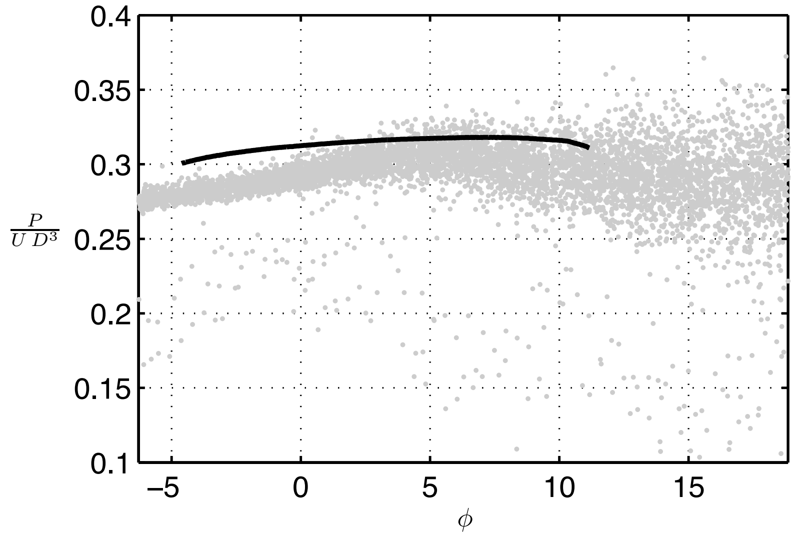


**Figure 12. Evolution of the linear impulse $P = \pi \int \omega_\varphi \, r^2 \, dr \, dz$: experimental results (grey bullets), DNS of the jet (solid)**

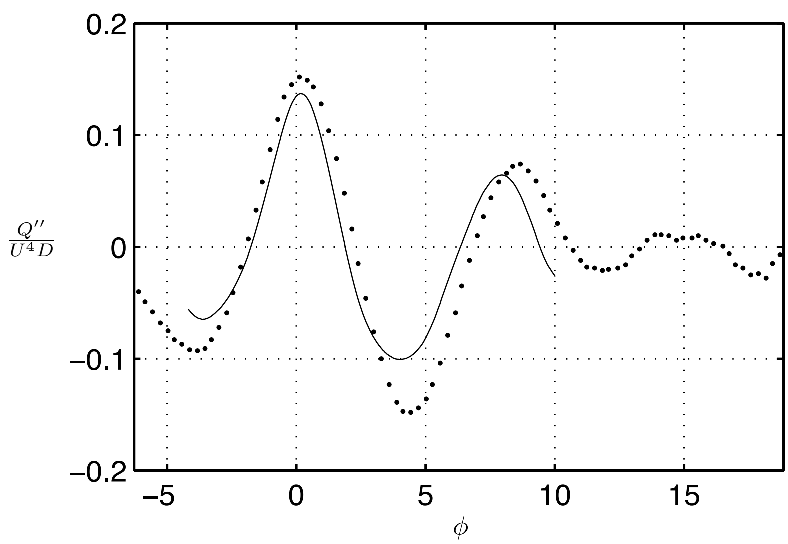


**Figure 13. Acoustic source term for the conservative analogy: experimental results (bullets), DNS of the jet with improved post-processing (solid).**

## VI. Conclusions

In this work, we performed the DNS of part of an experiment (isolated vortex rings) at a much higher Reynolds number than the previous studies (see Detandt et al.[2]). The obtained vorticity and velocity field thus represents a "perfect" experiment. It is observed that the global flow diagnostics (circulation, impulse, kinetic energy) are consistent with that of the experiment, which also further validates the numerical simulation of the flow. The obtained aeroacoustic source term is in fair agreement with the experimental results but there are some discrepancies in both amplitude and frequency. Indeed, the dynamics of an isolated pair of vortex rings are not those of such a pair as part of a complete jet; this can explain these discrepancies. The DNS of an axisymmetric jet with the same physical parameters as those of the experiment was then also simulated in order to better reproduce the experiment. The global flow diagnostics agree also quite well with the experimental data. With a basic vortex tracking algorithm, it was shown that the peak amplitude of the aeroacoustic source term is in better agreement with the experimental data than in the case of isolated vortex rings. In the jet, the signal processing is quite challenging: after the pairing, it is quite hard to isolate the evolution of the merged vortex pair in a moving window. This leads to numerical difficulties to obtain the signal on a longer time period. An improved vortex patch tracking algorithm was implemented which improves greatly the acoustic results. Recall also that, in the experiment at this high Reynolds number, the jet will be subjected to azimuthal instabilities which will eventually trigger turbulence. This cannot be simulated using our axisymmetric 2D code and using a 3D code would be required. Using the conservative aeroacoustic analogy based on vorticity will also allow to use 3-D hybrid Lagrangian-Eulerian codes (e.g. the vortex particle-mesh method VPM, also called VIC, see Cocle et al.[1] ) to perform aeroacoustics studies on more complex configurations and turbulent flows.

## VII. Acknowledgements

The simulations were done using the facilities of the Calcul Intensif et Stockage de Masse (CISM) on the UCL Lemaître and hmem clusters funded by Fond National de Recherche Scientifique (FNRS) under a FRFC Project and by UCL (Fonds Spéciaux de Recherche). The results were obtained in the framework of the SINUS project funded by the European commission FEDER funds and the Région Wallonne of Belgium. M.Duponcheel is a FNRS postdoctoral researcher.

## References

[1]Cocle R., Daeninck G., Winckelmans G., Combining the vortex-in-cell and parallel fast multipole methods for efficient domain decomposition simulations,*Journal of Computational Physics*, **227** Issue 21, November, 2008.

[2]Detandt Y., Degrez G., Schram C., Jet flow aeroacoustics at Re=14000 Comparison between experimental and numerical simulations, in proceedings of 28th AIAA Aeroacoustics Conference, (2007).

[3]Iafrati A. Riccardi G. A numerical evaluation of viscous effects on vortex induced noise. *Journal of Sound and Vibration*, 196:129–146(18), 1996.

[4]Kambe T., Minota T., Sound radiation from vortex systems, *Journal of Sound and Vibration* **74** (1) (1981) 6172.

[5]Lamb H., Hydrodynamics, 6th ed. Cambridge University Press, London, 1932.

[6]W. Mohring, On vortex sound at low Mach number, *Journal of Fluid Mechanics* **85** (1978) 85691.

[7]A.Powell,Theory of vortex sound, *Journal of the Acoustical Society of America* **36**(1)(1964) 177195.

[8]Schram, C., Hirschberg, A., Application of vortex sound theory to vortex-pairing noise: sensitivity to errors in flow data, *Journal of Sound and Vibration*, **266**, (2003).

[9]Schram, C., Taubitz, S., Anthoine, J., Hirschberg, A., Theoretical/empirical prediction and measurement of the sound produced byvortex pairing in a low Mach number jet, *Journal of Sound and Vibration*, **281**, (2005).

[10]R. Verzicco, A. Iafrati, G. Riccardi, and M. Fatica. Analysis of the sound generated by the pairing of two axisymmetric co-rotating vortex rings. *Journal of Sound and Vibration*, **200**(3):347 – 358, 1997.